Supporting Information

Formation Mechanism and Porosity Development in Porous Boron Nitride

Anouk L'Hermitte [1,2], Daniel M. Dawson [3], Pilar Ferrer [4], Kanak Roy [4,†], Georg Held [4], Tian Tian [1], Sharon E. Ashbrook [3] and Camille Petit [1*]*

[1] Barrer Centre, Department of Chemical Engineering, Imperial College London, London SW7 2AZ, United Kingdom

[2] Department of Materials, Imperial College London, London SW7 2AZ, United Kingdom

[3] School of Chemistry, EaStCHEM and Centre of Magnetic Resonance, University of St. Andrews, North Haugh, St. Andrews, Fife KY16 9ST, United Kingdom

[4] Diamond Light Source Ltd., Diamond House, Harwell Science and Innovation Campus, Didcot OX11 0DE, United Kingdom

[†] Current address: Department of Chemistry, Banaras Hindu University, Varanasi, Uttar Pradesh 221005, India

* Corresponding authors: Camille Petit (camille.petit@imperial.ac.uk, +44 (0)20 7594 3182); Sharon E. Ashbrook (sema@st-andrews.ac.uk, +44 (0)13 3446 3779)

1. Chemical aspects of the individual precursors, the initial mixture of precursors and carbon nitride

The theoretical FTIR spectrum for the initial mixture of reagents was calculated using the molar quantities of each reagent used in the synthesis (molar ratios BA:M:U = 1:1:5) and neglecting any interaction between them.

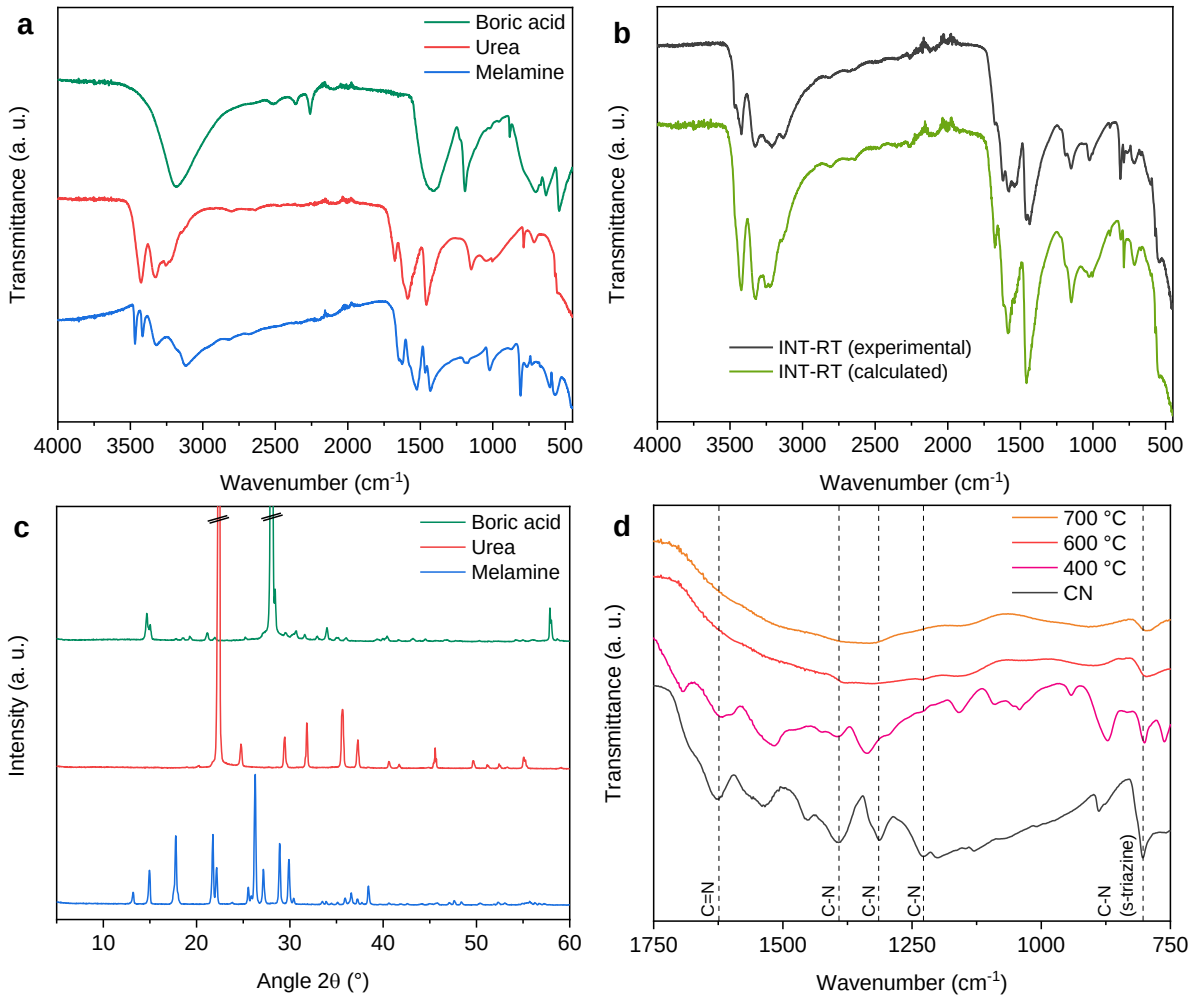

Figure S1. (a) FTIR spectra for each individual precursor. (b) FTIR spectra for INT-RT based on measurement ("experimental") and calculation ("calculated"). (c) XRD patterns for each individual precursor. (d) FTIR spectra for carbon nitride (CN) in comparison with INT-400, INT-600 and INT-700.

Table S1. Atomic composition derived from XPS analysis and calculated atomic composition for sample INT-RT corresponding to the initial mixture of reagents (BA:M:U = 1:1:5). Note: H atoms are not detected in XPS.

Atom	Calculated quantity (%at)	Measured quantity (%at)
B	3	14
N	49	37
O	24	28
C	24	22

2. Impact of dwell time during the synthesis of porous BN

Porous BN products obtained before and after a 3.5 h dwell time at 1050 °C were characterised in FTIR, XRD, XPS and N_2 sorption to investigate the potential differences in chemistry and porosity.

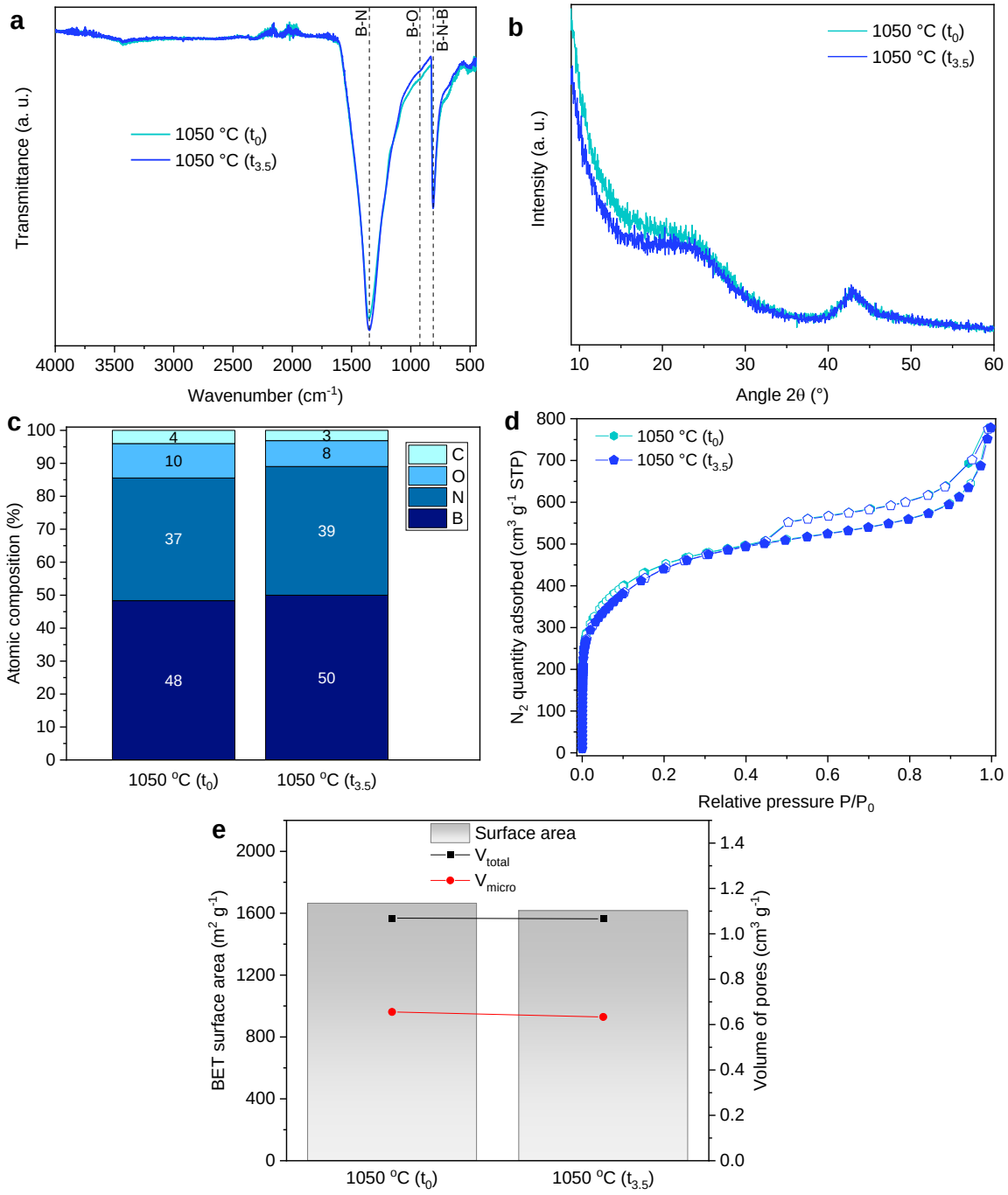

Figure S2. (a) FTIR spectra, (b) XRD patterns, (c) atomic composition derived from XPS, (d) N_2 sorption isotherms at –196 °C (full symbols = adsorption; open symbols = desorption) and (e) associated textural parameters for porous BN obtained at 1050 °C before and after 3.5 h dwell time.

3. ^{11}B MQMAS spectra of selected intermediates

Figure S3 shows the ^{11}B MQMAS NMR spectra (after shearing and referencing δ_1 as described in the main text) of INT-600, INT-700, INT-800 and INT-1050-t_0. Note that, to reduce spectral acquisition time, a narrow F_1 sweep width was chosen, such that the signals for tetrahedral B species are folded and should appear at much lower δ_1 values.

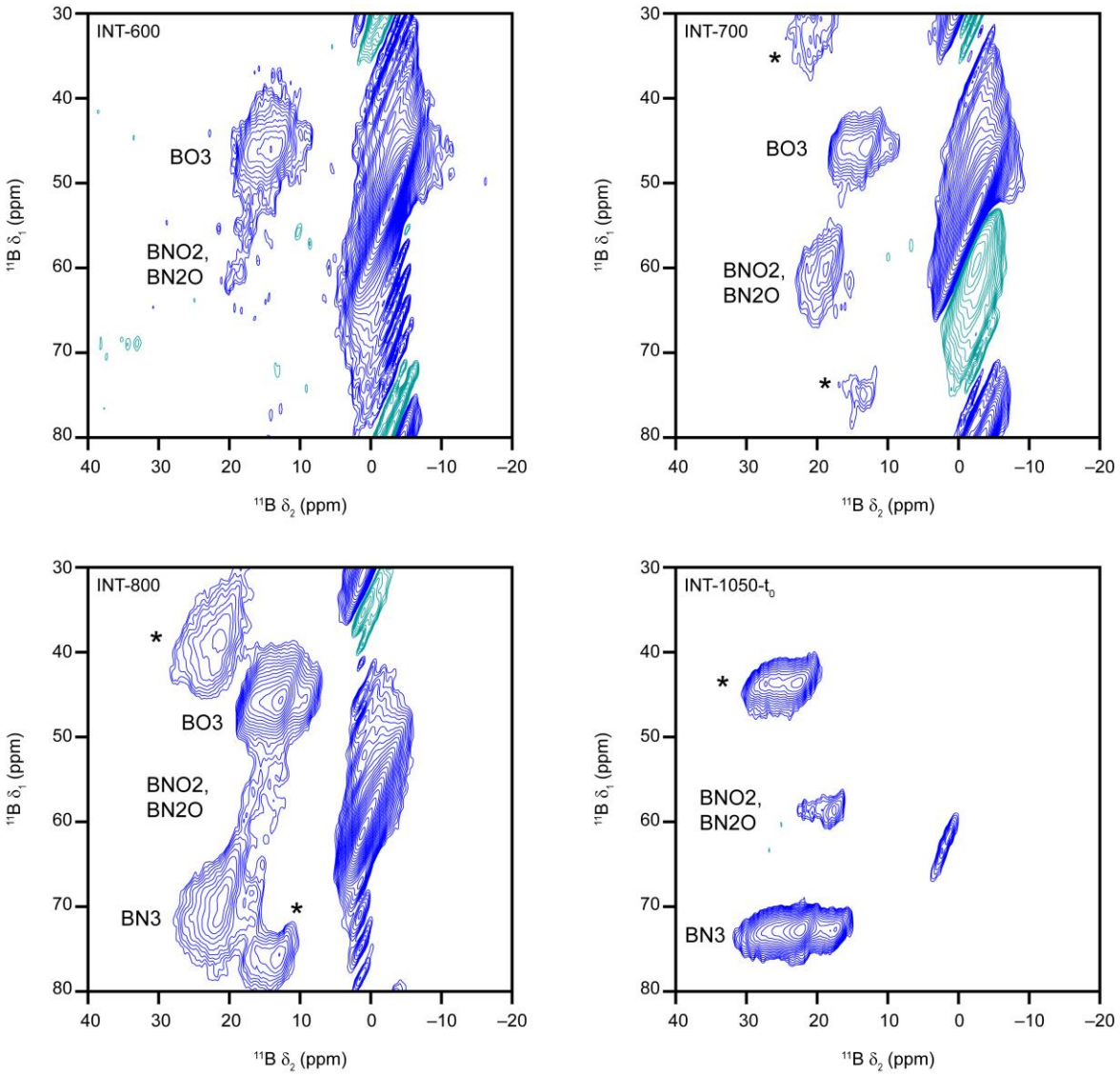

Figure S3. ^{11}B (14.1 T, 10 kHz MAS) MQMAS NMR spectra of selected intermediates. The resonances for trigonal B species are assigned and spinning sidebands are marked *. Contours are coloured with blue = positive, teal = negative.

4. Using DFT calculations to assign ^{11}B signals

Figure S4 shows the calculated ^{11}B δ_{iso} for the various models of N and O arrangements around B (see structures in the insets). Note that for the tetrahedral B species, simple clusters of the formula $[B(NH_2)_n(OH)_{4-n}]^-$ were used, whereas for trigonal B, a slightly larger model, approximating the structure of BN was used. However, these models tended to distort significantly on optimisation (the under-bonded N atoms favouring sp^3 rather than sp^2 hybridisation), and it was not possible to embed a tetrahedral B species in these small models.

The computed δ_{iso} values allow assignment of the NMR resonances from trigonal B species as discussed in the main text. However, for the tetrahedral B species, while δ_{iso} varies systematically with the number of bonded N and O, this is over a much smaller shift range and definitive assignment of the various tetrahedral B species observed in this study was not possible.

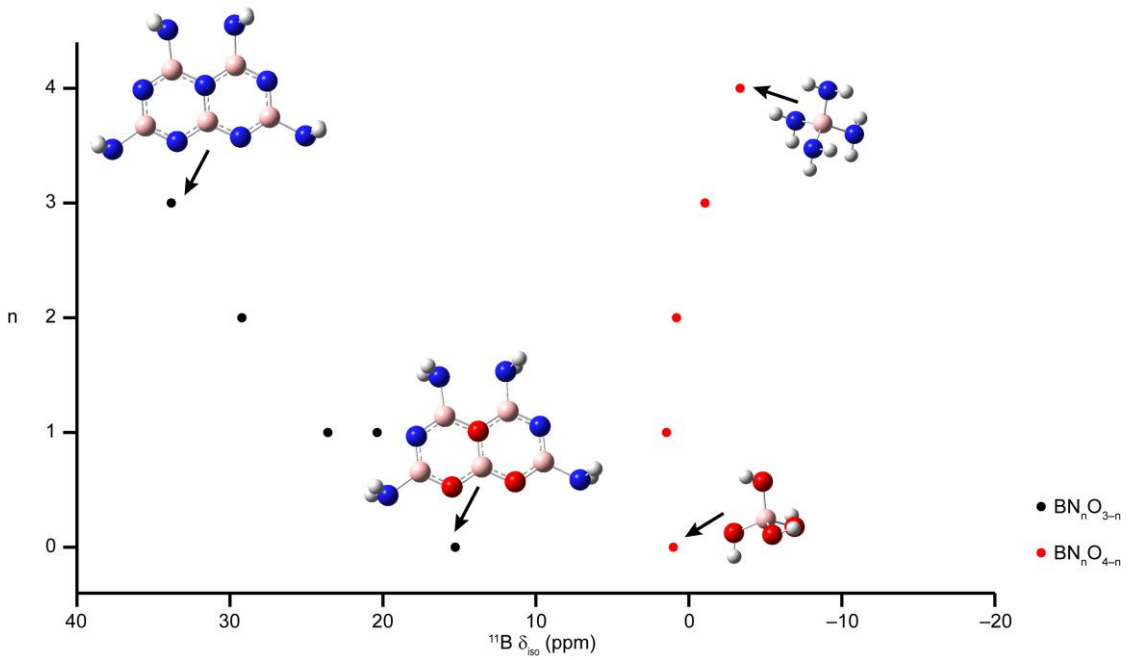

Figure S4. Plot of calculated ^{11}B δ_{iso} as a function of number of bonded nitrogen atoms (n) for tetrahedral BN_nO_{4-n} (red points, $0 \leq n \leq 4$) and trigonal BN_nO_{3-n} (black points, $0 \leq n \leq 3$) species. Examples for n = 0 and n = 3 or 4 input structures are shown, with atoms coloured B = pink, N = blue, O = red and H = white.

5. ^{11}B MAS NMR spectrum of boron oxide

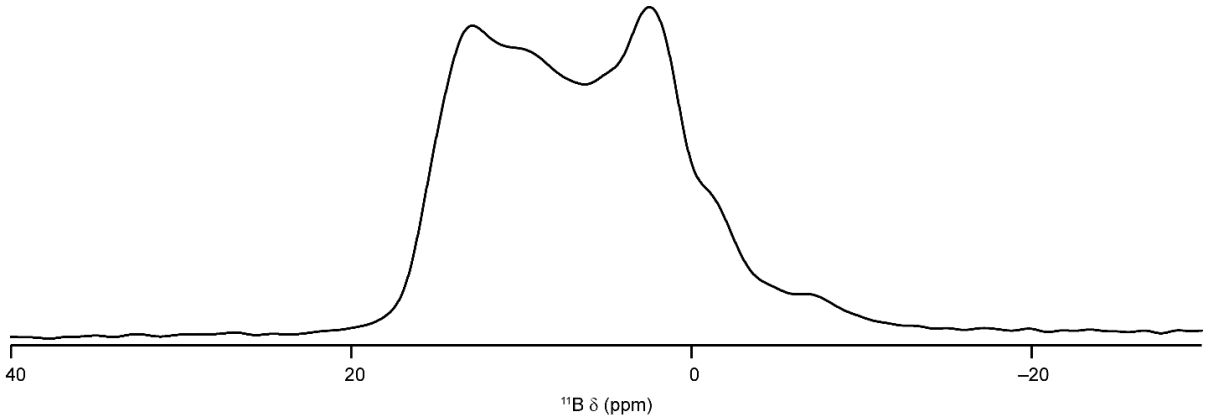

Figure S5. ^{11}B MAS NMR spectrum of B_2O_3, showing that the material is predominantly trigonal B. The spectrum was recorded using a Bruker Avance III spectrometer equipped with a wide-bore 9.4 T superconducting magnet (^{11}B Larmor frequency of 128.4 MHz) and a standard Bruker 4-mm MAS probehead. The sample was ground and packed into a zirconia rotor, and rotated about an axis inclined at the magic angle at a rate of 14 kHz. Spectra were acquired using a single soft pulse ($\nu_1 \approx 20$ kHz) of short flip angle ($\beta \approx 7°$). Signal averaging was carried out for 32 transients with a recycle interval of 60 s. Chemical shifts are shown relative to $BF_3.Et_2O$ using BPO_4 ($\delta = -3.3$ ppm) as a secondary solid reference.

6. ^{13}C NMR spectra

Figure S6 shows the ^{13}C NMR spectra for selected intermediates, compared with pure C_3N_4. It can be seen that condensation towards carbon nitride-like species starts at relatively low temperature but is not complete even by 600 °C.

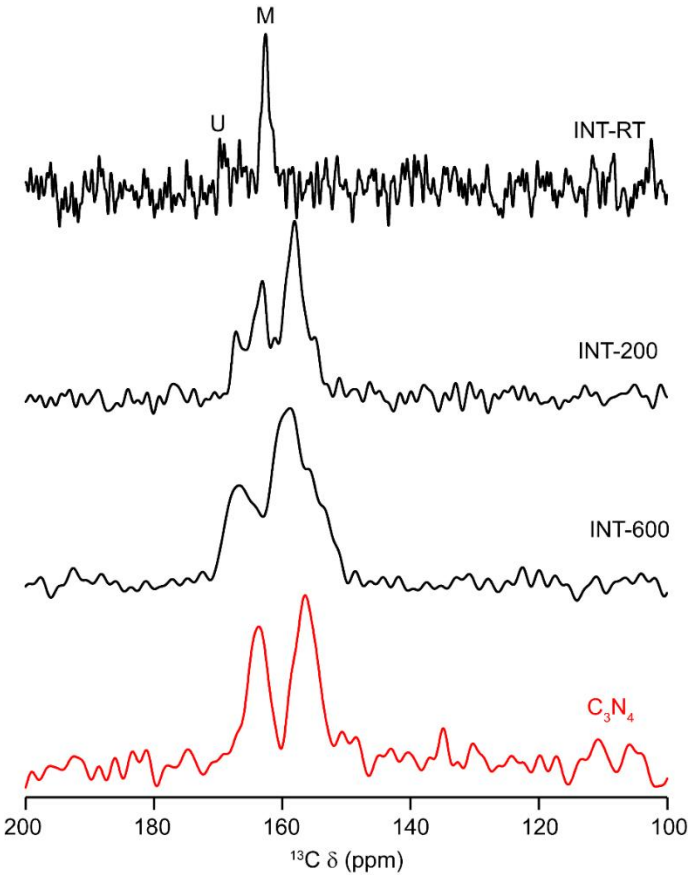

Figure S6. ^{13}C (9.4 T, 12.5 kHz MAS) NMR spectra of the indicated intermediates (black) and carbon nitride C_3N_4 (red). Owing to the very slow longitudinal relaxation for urea, the signal (marked U) is much lower in intensity, relative to the melamine (M) signal, than might be expected.

7. O-K edge NEXAFS

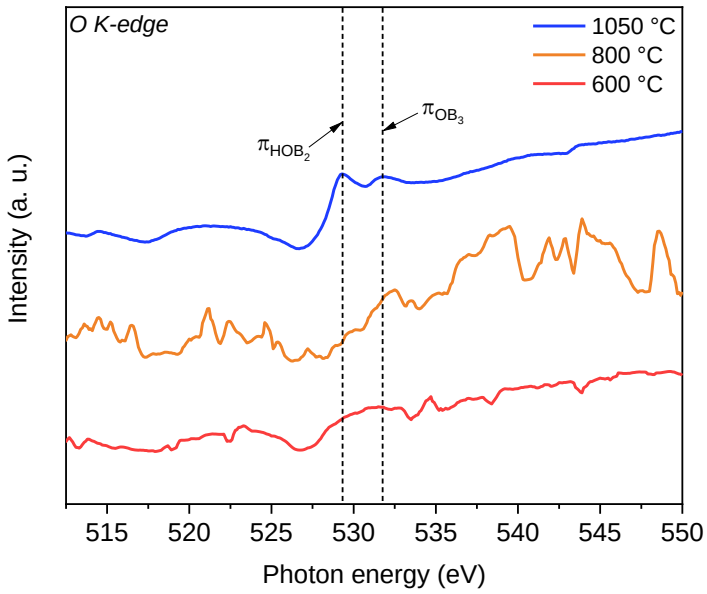

Figure S7. NEXAFS O K-edge spectra for the intermediates at 600 °C, 800 °C and the final product BN-1050-$t_{3.5}$.

8. Roles of urea and melamine as N-precursors

The choice of precursors is of paramount importance to form porous BN, based on the gaseous species being released (Figure S8). Although using either melamine or urea allows to produce porous BN with boric acid, a previous study showed that high hierarchical porosity in porous BN derives from complex thermal degradation patterns of precursors.[1] Herein, we will investigate whether melamine and urea play the roles of chemical precursors or porogens. We carried out TG analyses in N_2 for each reagent individually, as well as mixtures of boric acid (BA) with either urea (U) or melamine (M), or both at a time (Figure S7b). The boric acid to N-precursor molar ratios were kept constant: BA:M (1:1) and BA:U (1:5). TG-MS was done in parallel to survey the gases released by each combination of precursors and identify the source of porogens mentioned earlier (Figure S8c-f). After these experiments, we analysed the residues using FTIR spectroscopy to assess whether BN formed with each combination of reagents (Figure S8a). We obtained BN in all cases, but with traces of B-O and O-H, when using urea and melamine and with significant boron oxide B_2O_3 and other B-O compounds when using melamine only. This is most likely due to the lower B:N ratio in the case of melamine-based synthesis. TGA showed that the degradation profiles of the mixtures of reagents did not strictly follow the combination of each reagent's weight loss since additional reactions occurred (Figure S8b).

Thanks to TG-MS, we reported the main species released during the synthesis: ammonia NH_3, water H_2O, hydrogen cyanide HCN and carbon dioxide CO_2 (Figure S8c-f). Firstly, we observed that the gas release profiles were more complex when both N-containing precursors were used, with additional release peaks that would lead to enhanced porosity.[1] Ammonia release with both N-containing precursors roughly corresponded to the releases observed with either melamine or urea alone with boric acid (Figure S8c). While water release also followed

the pattern for each N-containing precursor, an additional peak was observed above 900 °C (Figure S8d), corresponding to the removal of O impurities and the formation of purer BN, as observed in XPS (Figure 2b). When both melamine and urea were used, we observed a continuous HCN release from 150 °C, which corresponded to the degradation of urea followed by the condensation of melamine into melem, leading to the formation of carbon nitride before 600 °C (Figure S8e). In the temperature range 700 – 800 °C corresponding to the porosity development with porogens HCN and CO_2, HCN was mainly released when melamine was used, either with or without urea (Figure S8e). In parallel, a significant release of CO_2 was observed only when both N-precursors were used (Figure S8f). This confirms that both melamine and urea are needed to enhance surface area and porosity in porous BN via the formation of intermediates (e.g., melem, carbon nitride) releasing HCN and CO_2, the main porogen agents.

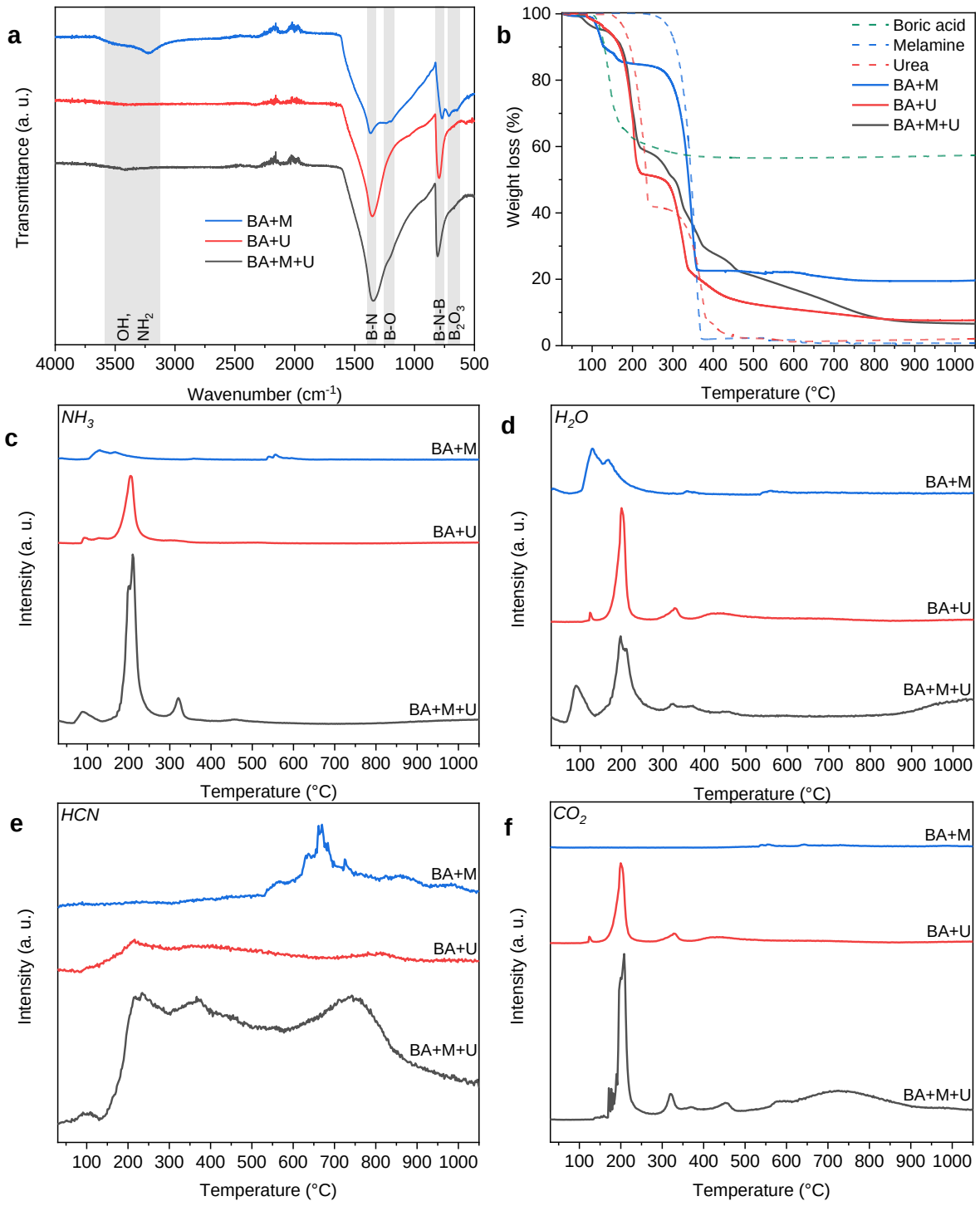
a
Transmittance (a. u.)
Wavenumber (cm-1)
OH, NH2
B-N
B-O
B-N-B
B2O3
BA+M
BA+U
BA+M+U
b
Weight loss (%)
Temperature (°C)
Boric acid
Melamine
Urea
BA+M
BA+U
BA+M+U
c
NH3
Intensity (a. u.)
Temperature (°C)
d
H2O
e
HCN
f
CO2

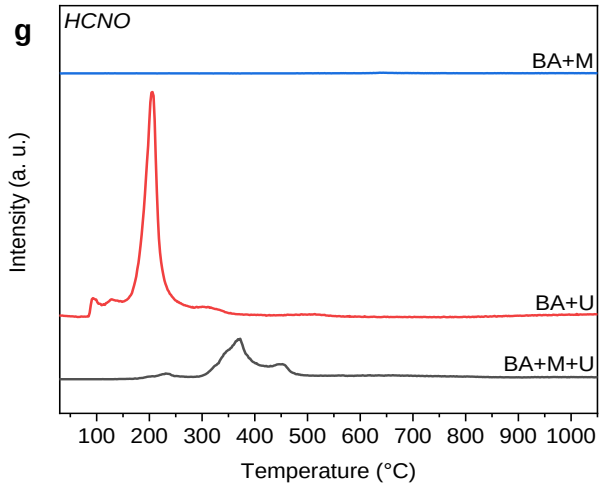

Figure S8. (a) FTIR spectra of residual products obtained after TG-MS with mixtures of boric acid (BA), urea (U) or/and melamine (M) with molar ratios of: BA:M = 1:1; BA:U = 1:5; and BA:M:U = 1:1:5. (b) TGA in N_2 for each reagent individually and the mixtures of reagents. (c-g) Mass spectra obtained in TG-MS for the different mixtures of reagents with the gaseous species: (c) Ammonia NH_3 (m/z = 17); (d) Water H_2O (m/z = 18); (e) Hydrogen cyanide HCN (m/z = 27); (f) Carbon dioxide CO_2 (m/z = 44); (g) HCNO (m/z = 43).